NANO LETTERS

2003
Vol. 3, No. 1
101−105

High Energy Excitations in CdSe Quantum Rods

Jingbo Li* and Lin-wang Wang

NERSC, Lawrence Berkeley National Laboratory, Berkeley, California 94720

Received October 26, 2002; Revised Manuscript Received November 11, 2002

ABSTRACT

The plane-wave pseudopotential method is used to calculate the high energy exciton states of large CdSe quantum rods, including spin–orbital coupling and screened electron–hole Coulomb interaction. Theoretical ground exciton energies of colloidal CdSe quanutm rods and wires are in good agreement with recent experiment. In addition to photoluminescence spectra, our results also show strong polarization in the absorption spectra of quantum rods, in contrast to spherical quantum dots. The absorption peaks as functions of the ground exciton energy are compared with experimental results.

1. Introduction. New fabrication methods have enabled the synthesis of high-quality CdSe quantum rods (the size distribution is typically 5% in diameter and 10% in length).[1,2] Since then, the shape effects of semiconductor nanocrystals have found many applications, such as in lasers,[3] biological labels,[4] and solar cells.[5] Size-dependence of the optical properties of CdSe spherical quantum dots has been studied extensively.[6−8] The band gap and oscillator strength can be tuned by the change of quantum dot size. However, nanocrystal shape can also significantly alter the optical properties of nanocrystals. For example, a recent experiment has found that the lack of a large overlap between absorption and emission spectra in CdSe quantum rods can improve the efficiency of light-emitting diodes (LEDs) since it reduces reabsorption.[9,10] Theoretically, semiconductor quantum rods provide a good opportunity to study the shape-dependent electronic and optical properties and the transition from zero-dimensional quantum dots to one-dimensional quantum wires.

Several theoretical approaches have been applied to treat the electronic level structure of spherical CdSe quantum dots. For example, both effective-mass theory[11−15] and empirical pseudopotential calculation[16−20] can be used successfully to describe the electronic states and optical properties of spherical CdSe quantum dots. However, the theoretical treatments of the shape effect on electronic structure of colloidal nanocrystals are scarce. Recently Hu et al. have calculated the electronic structure of CdSe quantum rods by the pseudopotential method.[9,10] The dependencies of electronic states on the length and diameter are studied. Highly linearized polarization is found in photoluminescence (PL) spectra, and the result is confirmed by experiment.[9] However, that work is concentrated on band edge states and PL spectra. Recently, the interest has been shifted to high excited states of colloidal CdSe quantum rods.[21,22] By changing the diameter of the rods, some high-energy excitonic transitions have been resolved.[22] It is also found that the absorption spectra for CdSe quantum rods are also linearly polarized.[21] These call for new theoretical investigations. In this work, we will use the pseudopotential method to study the absorption spectra and their polarizations of CdSe quantum rods. We will also compare the absorption spectra peaks to the recent experimental photoluminescence excitation (PLE) results.

2. Theory. The direct diagonalization of the pseudopotential Hamiltonian method has two steps: the single-particle problem and the electron−hole interaction problem.

The Single-Particle Problem. In the first step, we solve the single-particle Schrodinger equation for the wave function $\psi(\mathbf{x})$ (here, $\mathbf{x} = (\mathbf{r},\sigma)$ and $\sigma = \uparrow,\downarrow$ is the spin variable):

$$\left\{-\frac{1}{2}\nabla^2 + \sum_{n,\alpha} v_\alpha(|r - R_{n,\alpha}|)\right\}\psi_i(x) = \epsilon_i\psi_i(x) \qquad (1)$$

Here $v_\alpha(r)$ is the screened atomic pseudopotential of type α at position $R_{n,\alpha}$. The pseudopotential $v_\alpha(r)$ contains a local part and a nonlocal part that includes spin−orbit interaction. $v_\alpha(r)$ was previously obtained by "inverting" the self-consistently calculated ab initio bulk total potentials of various CdSe crystals. This ensures that the wave functions have ab initio qualities. Furthermore, special attention is directed at obtaining experimental effective masses and bulk band structures throughout the Brillouin zone. This is particularly important as rod orbitals are consistent with the bulk wave functions of the whole Brillouin zone. Equation 1 is solved for a 1000-atom quantum rod using the linear scaling "folded spectrum method" (FSM).[17,20] This method obtains directly the eigen solutions of the band edge states

10.1021/nl020231z CCC: $25.00
Published on Web 12/03/2002

without having to solve for the many states below the band gap. A parallel program called *Escan* is used in the current calculation. This program uses a parallel FFT, and a real space implementation of the nonlocal potential in eq 1. The computations were carried out on the supercomputers in the National Energy Research Scientific Computing Center (NERSC).

The Electron−Hole Interaction Problem. In the second step, we calculate the exciton transition energy as

$$E_{i,j} = \epsilon_{j,c} - \epsilon_{i,v} - J_{ij} \tag{2}$$

where J_{ij} is the Coulomb energy between the electron and hole. Here we have neglected the small exchange interaction and correlation effects. J_{ij} is calculated as

$$J_{i,j} = \int\int \frac{|\psi_{i,v}(x_1)|^2 |\psi_{j,c}(x_2)|^2}{\epsilon(r_1 - r_2)|r_1 - r_2|} \, \mathrm{d}^3x_1 \, \mathrm{d}^3x_2 \tag{3}$$

Unlike the case in bulk exciton, here the electron and hole are spatially close to each other, so the distance-dependent dielectric function is needed to obtain an accurate result. The screening $\epsilon(\mathbf{r}_1-\mathbf{r}_2)$ includes both the electronic and ionic contributions, which are described using the modified Penn model and the Haken formula, as discussed in ref 19.

The Optical Absorption Spectra and Polarization. The optical absorption intensity is obtained by summing over the dipole matrix elements coupling hole state (i,v) and electron state (j,c), i.e.,

$$I_{xyz}(E) = \sum_{i,j} \frac{4e^2}{3m^2c^2} |\langle \psi_{i,v} | P_{xyz} | \psi_{j,c} \rangle|^2 \, f(E - E_{ij}) \tag{4}$$

Here, $f(E-E_{ij})$ is a Gaussian broadening function, and P_{xyz} is the momentum operator with the subscript "*xyz*" denoting polarizations.

Structures and Surface Passivation. A rod shape is generated from the bulk wurtzite CdSe with a long axis along the crystallographic *c*-axis (which we will call the *z* axis in the following). We use bulk lattice constants $a = 4.3$ Å, $c = 7.001$ Å. Surface atoms with only one remaining bond have been systematically removed. In the laboratory-made CdSe quantum rods, the surface is capped with organic ligands. To simulate generic passivation we have placed positive (negative) short-range electrostatic potentials (called "ligand potentials") near the surface Se (Cd) atom. The details are described in ref 18.

3. Results and Discussion. We have calculated the energy levels of CdSe quantum rods and wires with the diameters of 2.0, 2.5, 3.0, and 3.8 nm, respectively. For 2 nm diameter quantum rods, we have calculated the aspect ratio ranging from 1.0 to 6.0. In these cases, our calculated electronic structures of the 2 nm quantum rods are the same as that shown in Figure 1 of ref 10. The two highest occupied levels are crossing as functions of the aspect ratio of the rods. The highest valence band energy levels arise from linear combinations of the atomic Se 4p orbitals. In spherical nanocrystals the Se p_{xy} orbitals have higher energies than the p_z, while in the quantum wire Se p_{xy} orbitals have lower energies than the p_z. The cross of these two energy levels happens when the rod aspect ratio is about 1.3. This level crossing results in a sharp transition from plan-polarized emission inside the *xy* plane to highly linear polarized emission along the *z* direction.[10] In Figure 1a, we show the electron−hole Coulomb energy for the exciton as a function of the aspect ratio for a 2 nm diameter quantum rod. Figure 1b shows the ground exciton energy including the Coulomb interaction as a function of the aspect ratio. We see that the shape affects the exciton energy most significantly when the aspect ratio is small. The biggest confinement happens at the aspect ratio of 1.0, i.e., the spherical dot. There the Coulomb energy can be as large as 0.35 eV. The ground exciton energy converges at aspect ratio of 3. We found that the high-energy exciton states will converge at about aspect ratio of 10.0. Figure 2 depicts the single-particle energy gap of CdSe quantum wires as a function of its diameter. The present calculations are shown by open-circles for four diameters of 2.0, 2.5, 3.0, and 3.8 nm, respectively. The triangles correspond to the experimental data by Katz et al. using scanning-tunneling measurement on single CdSe quantum rods at 4.2 K.[22] The dashed curve corresponds to the effective-mass calculation from ref 22. One can find a good agreement between pseudopotential calculation and experimental energy gap. To compare with the experimental data by Li et al.,[2] we have calculated two quantum rods with shapes that mimic the experimental quantum rod shapes: one of 3 nm in diameter and 11.3 nm in length, another of 3.8 nm in diameter and 9.8 nm in length. They contain 2540 and 3333 atoms, respectively. The calculated ground exciton energies (with Coulomb interaction included) and the corresponding experimental results are listed in Table 1. As one can see, the agreement with experiment is excellent.

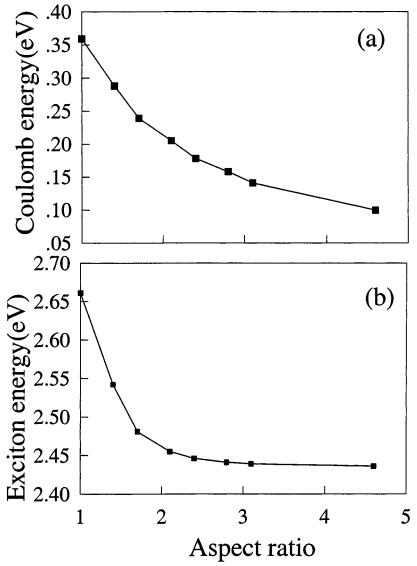

Figure 1. (a) Coulomb energy and (b) ground exciton energy of CdSe quantum rods as functions of the aspect ratio of rods. The diameter of quantum rods is 2 nm.

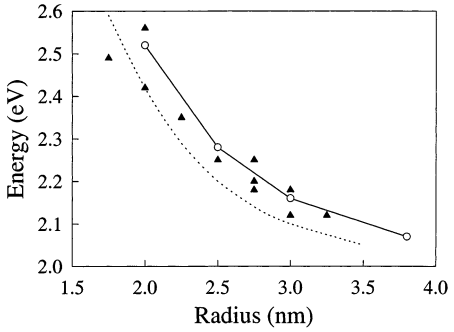

Figure 2. Comparison of the single-particle energy gap of CdSe quantum wires between theories and experiments. Dashed curve corresponds to effective-mass approximation from ref 22, triangles to the experimental data from ref 22 using scanning-tunneling measurement on single CdSe quantum rods at 4.2 K. Open circles correspond to present calculations. The solid line is a guide to the eye.

Table 1. Exciton Energies by Theoretical Calculation of CdSe Quantum Rods Compared with Experimental Data from Ref 2[a]

	diameter (nm)	length (nm)	exciton energy(eV)
present calc	3.0	11.3	2.18
expt (ref 2)	3.2	11.0±0.7	2.20
present calc	3.8	9.8	2.10
expt (ref 2)	3.8	8.6±0.8	2.12

[a] Screened electron−hole Coulomb energy is included in the calculation.

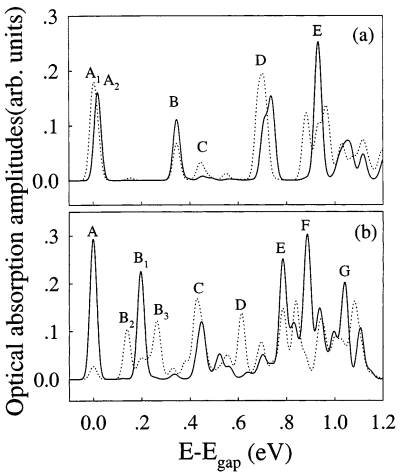

Figure 3. Theoretical optical transition spectra of CdSe quantum rods calculated using the screened pseudopotential Hamiltonian. Coulomb interaction has been taken into account in the calculaton. E_{gap} is the ground exciton energy. The solid-curve shows the *z*-direction polarized transition; the dotted curve shows *xy*-plane polarized transition. (a) The aspect ratio of the rod is 1, and (b) the aspect ratio of the rod is 3.1.

The calculated optical absorption spectra of CdSe quantum rods with 2 nm diameter are shown in Figure 3a,b for the aspect ratio of 1.0 (spherical quantum dots) and 3.1 (quantum rods), respectively. We can identify the transition peaks as A, B, C, D, E, F, G in Figure 3. Solid-curves show the *z*-direction polarized transitions, while the dotted curves show the averaged *xy*-plane polarized transitions. We denote the conduction band (CB) states as CB_n in increasing energy order from the conduction band minimum using $n = 1$, 2, ..., and denote the valence band (VB) states as VB_n in decreasing energy order from the valance band maximum using $n = 1,2,...$ The line shapes and intensities of the transition peaks in Figure 3a are consistent with previous calculations[19,20] for quantum dot systems. Group A peaks originate from the $VB_1 \rightarrow CB_1$ (A_1) and $VB_2 \rightarrow CB_1$ (A_2) transitions. The splitting between the A_1 and A_2 peaks corresponds to the crystal-field splitting by wurtzite structure in CdSe quantum dots. The B peak originates from $VB_5 \rightarrow CB_1$ and $VB_7 \rightarrow CB_1$ transitions. The strong D and E peaks involve high energy level transitions. For example, the D peak originates from $(VB_3,VB_4) \rightarrow (CB_2,CB_3,CB_4)$ transitions, while the E peak originates from $(VB_5,VB_6,VB_7) \rightarrow (CB_3,CB_4)$ transitions. The *xy*-plane polarized and *z*-direction polarized curves are similar in Figure 3a. Thus there is no strong polarization effect in a spherical quantum dot, although wurtrize structure is intrinsically asymmetric. In contrast, a high polarization of the absorption spectra is found in the quantum rod, as shown in Figure 3b. It shows strong polarization dependence up to 0.8 eV above the absorption edge. Beyond that, there are many peaks and the polarization effects are averaged out. The polarization dependence of the absorption spectra is confirmed by recent PLE experiment of single CdSe quantum rods.[21] In that experiment, it was found that the absorption coefficient depends on the exciting photon polarization at a given photon energy. However, based on our calculated results in Figure 3b, one can expect to see more rich experimental results by scanning the PLE excitation energy from the absorption edge. The polarization direction should change with the change of excitation energy. This is waiting for experimental confirmation. In Figure 3b, A and B_1 peaks originate from $VB_1 \rightarrow CB_1$ and $VB_2 \rightarrow CB_2$ transitions, respectively. Their transitions are from the *z*-direction polarization modes. B_2 and B_3 peaks involve *xy*-plane polarized transitions. Their intensities are weaker than that of the B_1 peak. They originate from the $VB_3 \rightarrow CB_1$ and $VB_4 \rightarrow CB_2$ transitions, respectively. In Figure 3b, the E, F, and G peaks also involve high-energy transitions. The E peak corresponds to $(VB_6,VB_{15}) \rightarrow (CB_6,CB_4)$ transitions. The F peak corresponds to $(VB_7,VB_{11}) \rightarrow (CB_7,CB_8)$ transitions. The G peak corresponds to $(VB_{14},VB_{19}) \rightarrow (CB_9,CB_6)$ transitions.

Recent experiments of PLE spectra for CdSe quantum rods with long length are reported by Katz et al.[22] To compare to their experiment, we have calculated the optical absorption spectra of CdSe quantum wires with diameters of 2.0, 2.5, 3.0, and 3.8 nm. The band gaps E_g are 2.52 eV, 2.3 eV, 2.22 eV, and 2.09 eV, respectively. To our knowledge this is the first theoretical calculation of optical absorption spectra of a CdSe quantum wire. The results are shown in Figure 4. The shape of main peaks in Figure 4 is similar to the idealized density of states of one-dimensional quantum wires.[23] In this calculation, 10 k_z points are used for each quantum wire to get the eigen energies and optical transition matrix elements, then linear interpolation is used to generate the results of 100 k_z points. This procedure gives well converged band structures and absorption spectra. The major transition peaks are assigned by the letters *a*−*e*. The connection of the peaks across different quantum wire sizes

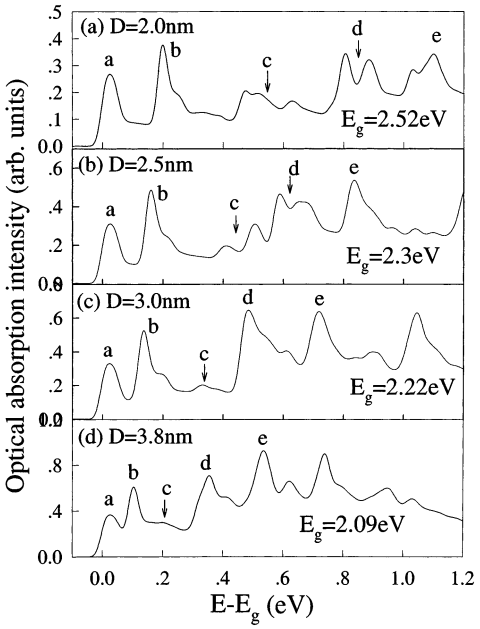

Figure 4. Theoretical excitonic transition spectra for four CdSe quantum wires with diameters of 2.0, 2.5, 3.0, and 3.8 nm from the top to bottom curves, respectively. E_g is the ground exciton energy. 20 meV Gaussion broading is used to generate the spectra. The major peaks are labeled from letter *a* to letter *e*. The region above peak *e* cannot be trusted since not enough hole stateds are calculated for that region.

is done by examining the symmetries of the initial and final single-particle states related to each peak. Some peaks might contain a few closely packed small peaks. For example, in Figure 4a,b, peaks *c* and *d* contain two or three peaks around the position. But if we use a Gaussian broadening function to fit these peaks, one can see that the separation peaks would become one peak. Thus, we only assigned a few large peaks (*a*−*e*) in the low energy region and use them to compare with experiment. Except peak *c*, all other peaks are originated from the Γ-point ($k_z = 0$) transition. At the Γ-point, peaks *a* and *b* are related to the $VB_1 \rightarrow CB_1$ and $(VB_2,VB_3) \rightarrow CB_1$ transitions, respectively. Peaks *d* and *e* include high-energy transitions. The main contribution to peaks *d* and *e* include transitions from $(VB_3,VB_4) \rightarrow (CB_2,CB_3)$ and $(VB_5,VB_6,VB_7,VB_8) \rightarrow (CB_2,CB_3)$, respectively. Unlike the other peaks, peak *c* originates from transitions at the shoulder of the band structure: $0.15(2\pi/c) < k_z < 0.2(2\pi/c)$.

Figure 5 plots the positions of above peaks (filled dots) and experimental PLE spectra results[22] (diamonds) as functions of the ground exciton energy. Our pseudopotential calculations show reasonable agreement with experimental results without any adjustable parameters. Especially the positions of peak *c* are in good agreement with the experiment. In ref 22, both PLE spectra and scanning-tunneling spectroscopy are used to study the electronic states of CdSe quantum rods. However, only PLE spectra can be compared directly with the calculated aborption spectra in Figure 5. There are not enough highly excited states of PLE spectra in ref 22. More experimental results are desired. For tunneling spectroscopy in ref 22, the experiment probes the energy difference between conduction band states. For E_g

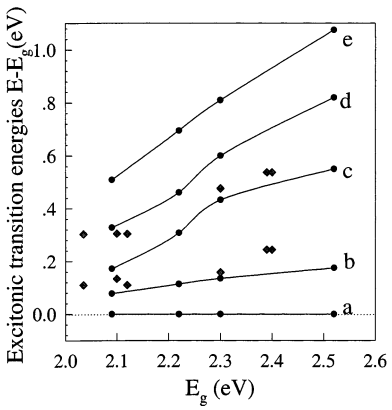

Figure 5. Transition energies (relative to the ground exciton state) vs the energy of the first ground exciton of CdSe quantum wires. Diamonds correspond to experimental data from ref 22 by PLE spectra. Theoretically predicted transition peaks are shown as filled dots, and the solid curves are guides for eys.

between 2.2 and 2.4 eV, the experimental CB_2-CB_1 energy is in the range of 0.5 and 0.7 eV. Our calculated energy difference of CB_2-CB_1 is in the same range, but slightly smaller by about 0.05 eV.

4. Conclusions. We have used a plane-wave empirical pseudopotential method to calculate the electronic structures and optical spectra of surface-passivated CdSe quantum rods and wires. We found that: (1) electron−hole Coulomb energies and exciton energies decrease when the aspect ratio of the rod increases; (2) our calculated ground exciton energies are in excellent agreement with the recent experimental PL energies for the same quantum rod shapes and sizes; (3) strongly linearized polarization exists in optical absorption spectra of CdSe quantum rods. This is in contrast with spherical shape CdSe quantum dots, and in agreement with recent experiment. New experiments can be carried out to confirm the calculated excitation energy dependence of the polarization. (4) The positions of the assigned high energy absorption peaks as functions of the ground exciton energies are in good agreement with the experiment. However, More experimental results are desired for comparison with our theoretical absorption spectra.

Acknowledgment. The authors thank Professor Paul A. Alivisatos for helpful discussions. This work was supported by the U.S. Department of Energy, OER-BES, under Contract No. KC0203010. This research used the resources of the National Energy Research Scientific Computing Center (NERSC), which is supported by the Office of Science of the U.S. Department of Energy.

References

(1) Peng, X.; Manna, L.; Yang, W. D.; Wickham, J.; Scher, E.; Kadavanich, A.; Alivisatos, A. P. *Nature* **2000**, *404*, 59.
(2) Li, L. S.; Hu, J.; Yang, W.; Alivisatos, A. P. *Nano Lett.* **2001**, *1*, 349.
(3) Kazes, M.; Lewis, D. Y.; Ebenstein Y.; Mokari, T.; Banin, U. *Adv. Mater.* **2002**, *14*, 317.
(4) Bruchez, M.; Moronne, M.; Gin, P.; Weiss, S.; Alivisatos, A. P. *Science* **1998**, *281*, 2013.
(5) Huynh, W. U.; Dittmer, J. J.; Alivisatos, A. P. *Science* **2002**, *295*, 2425.

(6) Alivisatos, A. P. *Science* **1996**, *271*, 933.
(7) Brus, L. E. *J. Chem. Phys.* **1984**, *80*, 4403.
(8) Murray, C. B.; Norris, D. J.; Bawendi, M. G. *J. Am. Chem. Soc.* **1993**, *115*, 8706.
(9) Hu, J.; Li, L. S.; Yang, W.; Manna, L.; Wang, L. W.; Alivisatos, A. P. *Science* **2001**, *292*, 2060.
(10) Hu, J.; Wang, L. W.; Li, L. S.; Yang, W.; Alivisatos, A. P. *J. Phys. Chem. B* **2002**, *106*, 2447.
(11) Norris, D. J.; Sacra, A.; Murray, C. B.; Bawendi, M. G. *Phys. Rev. Lett.* **1994**, *72*, 2612.
(12) Xia, J. B. *Phys. Rev. B* **1989**, *40*, 8500.
(13) Xia, J. B.; Li, J. B. *Phys. Rev. B* **1999**, *60*, 11540.
(14) Li, J. B.; Xia, J. B. *Phys. Rev. B* **2000**, *61*, 15880.
(15) Takagahara, T. *Phys. Rev. B* **1993**, *47*, 4569.
(16) Wang, L. W.; Zunger, A. *Phys. Rev. Lett.* **1994**, *73*, 1039.
(17) Wang, L. W.; Zunger, A. *J. Chem. Phys.* **1994**, *100*, 2394.
(18) Wang, L. W.; Zunger, A. *Phys. Rev. B* **1996**, *53*, 9579.
(19) Franceschetti, A.; Fu, H.; Wang, L. W.; Zunger, A. *Phys. Rev. B* **1999**, *60*, 1819.
(20) Wang, L. W.; Zunger, A. *J. Phys. Chem. B* **1998**, *102*, 6449.
(21) Chen, X.; Nazzal, A.; Goorskey, D.; Xiao, M.; Peng, Z. A.; Peng, X. *Phys. Rev. B* **2001**, *64*, 245304.
(22) Katz, D.; Wizansky, T.; Millo, O.; Rothenberg, E.; Mokari, T.; Banin, U. *Phys. Rev. Lett.* **2002**, *89*, 86801.
(23) Alivisatos, A. P. *J. Phys. Chem.* **1996**, *100*, 13226.

NL020231Z